Large-scale and multipolar anisotropies of cosmic rays detected at the Pierre Auger Observatory with energies above 4 EeV

Rogerio M. de Almeida, for the Pierre Auger Collaboration

Universidade Federal Fluminense

International Cosmic Ray Conference 2021 - 2021 / 07 / 15

The study of anisotropies is important to understand the origin of UHECR

- Dipolar or quadrupolar patterns expected in case of diffusive or quasi-rectilinear propagation from an anisotropic distribution of sources or diffusive propagation from the closest extragalactic source(s).

- Even for a pure dipole gradient at the entrance of the Galaxy, magnetic deflections are expected to give rise to higher-order multipoles, although with small amplitudes.

This work:

- We reconstruct **dipolar and quadrupolar** components through a combined Fourier analysis of the event rate in right ascension and azimuth and measure the **angular power spectrum** of events detected with energies above 4 EeV **(full efficiency of SD).**

- Data set composed of **150,688 events** detected by the surface detector with $\boldsymbol{\theta < 80^{\circ}}$ **(covering 85% of the sky, $\boldsymbol{\delta < 45^{\circ}}$)** from 01/01/2004 until 12/31/2020.

- Total accumulated exposure of **110,000 km^2 sr yr.**

Large scale: weighted harmonic analysis

- Search for harmonic modulation in right ascension and azimuth: $x = \alpha$ or ϕ
- Fourier coefficients of order k (1 or 2): $a_x^k = \frac{2}{\mathcal{N}} \sum_{i=1}^{N} w_i \cos(kx_i),\ b_x^k = \frac{2}{\mathcal{N}} \sum_{i=1}^{N} w_i \sin(kx_i)$
- amplitude $r_k^x = \sqrt{(a_k^x)^2 + (b_k^x)^2}$, phase $\varphi_k^x = \frac{1}{k} \tan^{-1} \frac{b_k^x}{a_k^x}$
- weights: small variations in coverage and tilt of the array

$$w_i = \left[\Delta N_{cell}\left(\alpha_i^0\right)\left(1 + 0.003 \tan\theta_i \cos(\phi_i - \phi_0)\right)\right]^{-1}$$

number of active detector cells

right ascension of the zenith of the observatory

average tilt of the array $\phi_0 = -30^\circ$

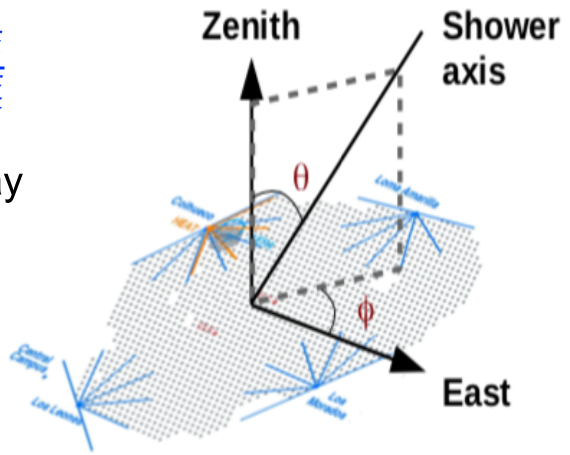

For dipolar modulation, $d_\perp \simeq \frac{r_1^\alpha}{\langle \cos\delta \rangle}$ **and** $d_z \simeq \frac{b_1^\phi}{\langle \sin\theta \rangle \cos l_{obs}}$

Dipole reconstruction

E (EeV)	N	$d_\perp$	d_z	d	$\alpha_d[°]$	$\delta_d[°]$	$\mathrm{P}(\geq r_1^\alpha)$
4-8	106, 290	$0.01^{+0.006}_{-0.004}$	-0.012 ± 0.008	$0.016^{+0.008}_{-0.005}$	97 ± 29	-48^{+23}_{-22}	1.4×10^{-1}
8-16	32, 794	$0.055^{+0.011}_{-0.009}$	-0.03 ± 0.01	$0.063^{+0.013}_{-0.009}$	95 ± 10	-28^{+12}_{-13}	3.1×10^{-7}
16-32	9, 156	$0.072^{+0.021}_{-0.016}$	-0.07 ± 0.03	$0.10^{+0.03}_{-0.02}$	81 ± 15	-43^{+14}_{-14}	7.5×10^{-4}
≥8	44, 398	$0.059^{+0.009}_{-0.008}$	-0.042 ± 0.013	$0.073^{+0.011}_{-0.009}$	95 ± 8	-36^{+9}_{-9}	5.1×10^{-11}
≥32	2, 448	$0.11^{+0.04}_{-0.03}$	-0.12 ± 0.05	$0.16^{+0.05}_{-0.04}$	139 ± 19	-47^{+16}_{-15}	1.0×10^{-2}

was 1.4×10^{-9} (ApJ 2020) and 2.6×10^{-8} (Science 2017)

Corresponds to 6.6σ

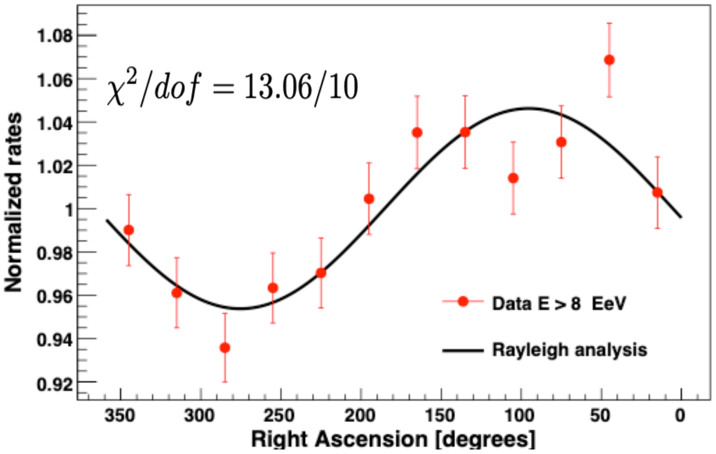

$E \geq 8$ EeV

Smoothed by a top-hat window with 45° of radius

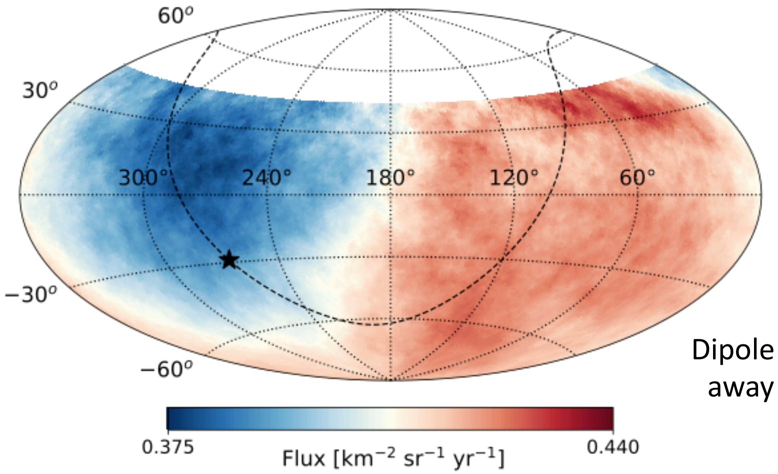

Dipole points $\sim 115^\circ$ away from the GC

Dipole reconstruction

E (EeV)	N	$d_\perp$	d_z	d	$\alpha_d[°]$	$\delta_d[°]$	$\mathrm{P}(\geq r_1^\alpha)$
4-8	106, 290	$0.01^{+0.006}_{-0.004}$	-0.012 ± 0.008	$0.016^{+0.008}_{-0.005}$	97 ± 29	-48^{+23}_{-22}	1.4×10^{-1}
8-16	32, 794	$0.055^{+0.011}_{-0.009}$	-0.03 ± 0.01	$0.063^{+0.013}_{-0.009}$	95 ± 10	-28^{+12}_{-13}	3.1×10^{-7}
16-32	9, 156	$0.072^{+0.021}_{-0.016}$	-0.07 ± 0.03	$0.10^{+0.03}_{-0.02}$	81 ± 15	-43^{+14}_{-14}	7.5×10^{-4}
≥8	44, 398	$0.059^{+0.009}_{-0.008}$	-0.042 ± 0.013	$0.073^{+0.011}_{-0.009}$	95 ± 8	-36^{+9}_{-9}	5.1×10^{-11}
≥32	2, 448	$0.11^{+0.04}_{-0.03}$	-0.12 ± 0.05	$0.16^{+0.05}_{-0.04}$	139 ± 19	-47^{+16}_{-15}	1.0×10^{-2}

was 1.4×10^{-9} (ApJ 2020) and 2.6×10^{-8} (Science 2017)

Corresponds to 6.6σ

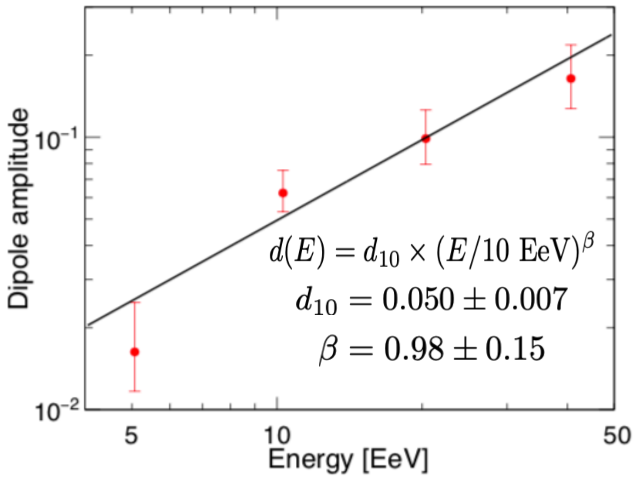

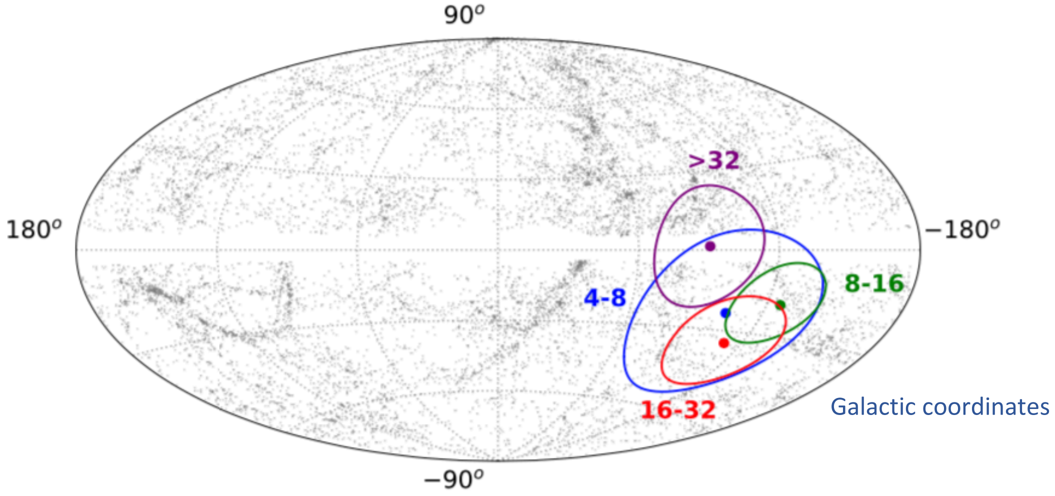

No clear trend in the evolution of dipole direction with energy

Dipole interpretation

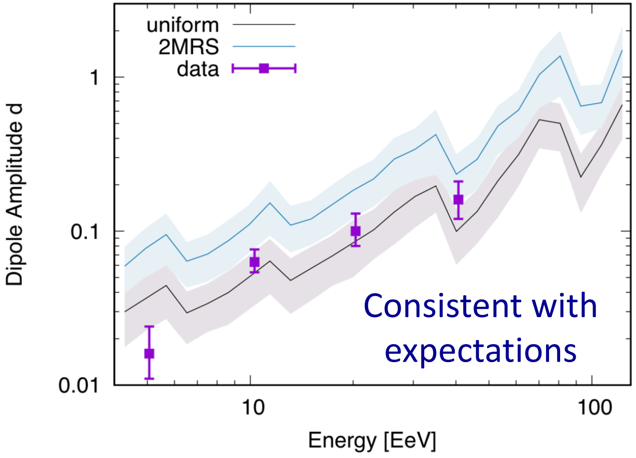

Models with mixed composition, $R_{max} = 6\ \mathrm{EV}$, source density $10^{-4}\ \mathrm{Mpc}^{-3}$ from PRD 92 (2015) 063014

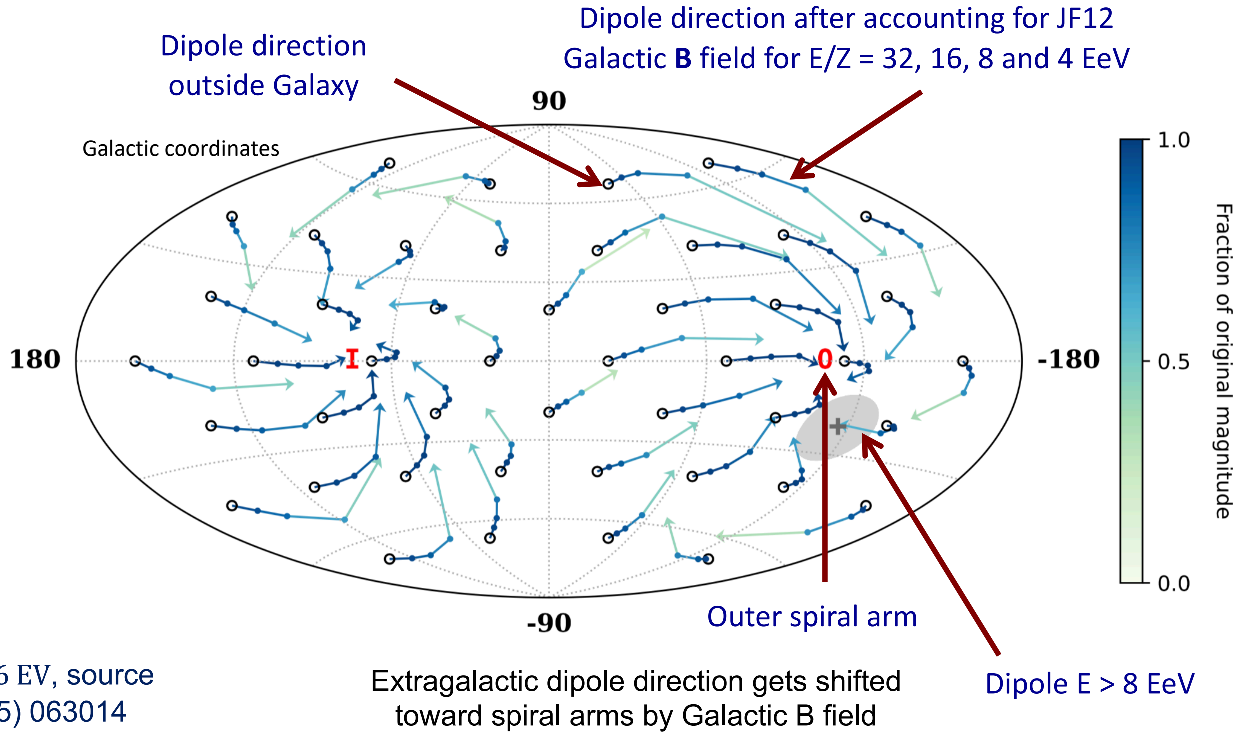

Extragalactic dipole direction gets shifted toward spiral arms by Galactic B field

Possibly due to the larger relative contribution from nearby sources to the flux at higher energies: extensive theoretical work (prediction and interpretation)

Giler et al. (JPhG 1980), Berezinsky et al. (A&A 1990), Harari et al. (PRD 2014), Harari et al. (PRD 2015), Globus & Piran (ApJL 2017), Wittkowski & Kampert (ApJL 2018), di Matteo et al. (MNRAS 2018), Hackstein et al. (MNRAS 2016), Hackstein et al. (MNRAS 2018), Ding et al. (ApJL 2021)

Dipolar + quadrupolar reconstruction

Energy [EeV]	d_i	Q_{ij}
4-8	$d_x = -0.008 \pm 0.007$	$Q_{zz} = 0.008 \pm 0.036$
	$d_y = 0.008 \pm 0.007$	$Q_{xx} - Q_{yy} = 0.004 \pm 0.026$
	$d_z = -0.008 \pm 0.021$	$Q_{xy} = -0.01 \pm 0.01$
		$Q_{xz} = -0.02 \pm 0.02$
		$Q_{yz} = -0.008 \pm 0.017$
8-16	$d_x = -0.005 \pm 0.013$	$Q_{zz} = 0.074 \pm 0.064$
	$d_y = 0.045 \pm 0.013$	$Q_{xx} - Q_{yy} = 0.02 \pm 0.05$
	$d_z = 0.01 \pm 0.04$	$Q_{xy} = 0.039 \pm 0.024$
		$Q_{xz} = -0.002 \pm 0.031$
		$Q_{yz} = -0.03 \pm 0.03$

Quadrupolar amplitudes not significant and dipole components consistent with those obtained by assuming a pure dipole

Energy [EeV]	d_i	Q_{ij}
16-32	$d_x = 0.05 \pm 0.02$	$Q_{zz} = -0.14 \pm 0.14$
	$d_y = 0.09 \pm 0.02$	$Q_{xx} - Q_{yy} = 0.17 \pm 0.09$
	$d_z = -0.15 \pm 0.07$	$Q_{xy} = -0.05 \pm 0.04$
		$Q_{xz} = 0.12 \pm 0.06$
		$Q_{yz} = 0.06 \pm 0.06$
≥ 32	$d_x = -0.12 \pm 0.05$	$Q_{zz} = -0.17 \pm 0.26$
	$d_y = 0.11 \pm 0.05$	$Q_{xx} - Q_{yy} = 0.43 \pm 0.17$
	$d_z = -0.22 \pm 0.13$	$Q_{xy} = 0.10 \pm 0.09$
		$Q_{xz} = -0.12 \pm 0.11$
		$Q_{yz} = 0.13 \pm 0.11$
≥ 8	$d_x = -0.001 \pm 0.011$	$Q_{zz} = 0.02 \pm 0.06$
	$d_y = 0.06 \pm 0.01$	$Q_{xx} - Q_{yy} = 0.08 \pm 0.04$
	$d_z = -0.03 \pm 0.03$	$Q_{xy} = 0.02 \pm 0.02$
		$Q_{xz} = 0.02 \pm 0.03$
		$Q_{yz} = -0.003 \pm 0.026$

Quadrupolar amplitudes not significant and dipole components consistent with those obtained by assuming a pure dipole

Angular Power Spectrum

- Same approach as JCAP 06 (2017) 026;
- Same data set used for Rayleigh analysys
- Data set 2.15 x larger than JCAP sample:

$$\Phi(\mathbf{n}) = \frac{N}{4\pi f_1} W(\mathbf{n})\left[1 + \Delta(\mathbf{n})\right]$$

$$\langle \mathrm{C}_\ell \rangle = \sum_{\ell_1} M^{-1}_{\ell\ell_1} \left\langle \tilde{\mathrm{C}}_\ell \right\rangle - \frac{4\pi f_1^2}{N f_2}$$

$$M_{\ell\ell_1} = \frac{2\ell_1 + 1}{4\pi} \sum_{\ell_2} (2\ell_2 + 1) \mathrm{W}_{\ell_2} \begin{pmatrix} \ell & \ell_1 & \ell_2 \\ 0 & 0 & 0 \end{pmatrix}^2$$

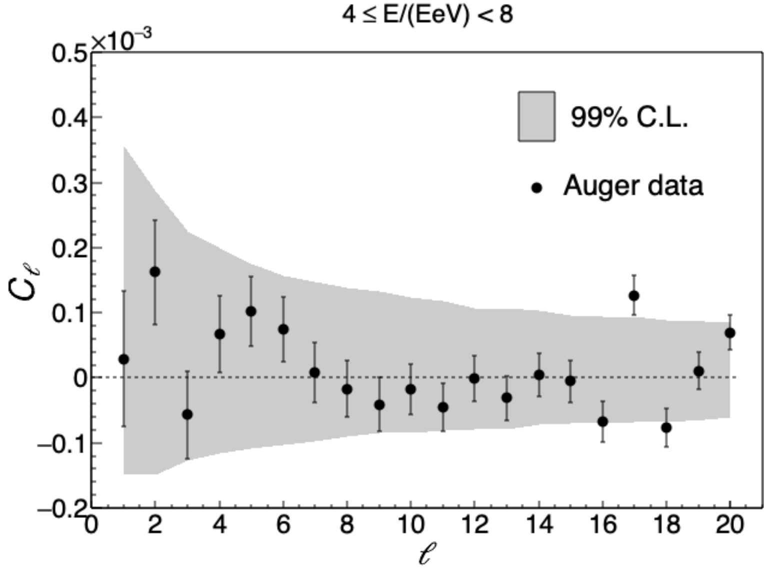

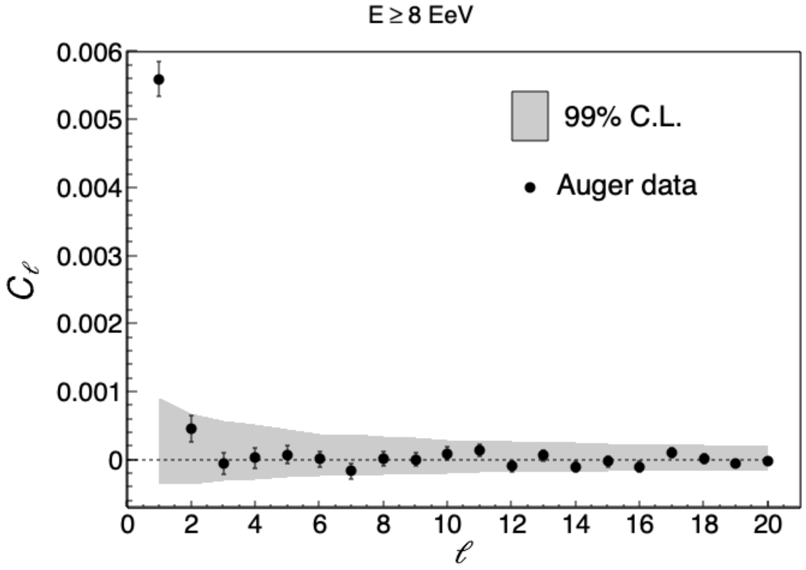

Angular Power Spectrum

$$\Phi(\mathbf{n}) = \frac{N}{4\pi f_1} W(\mathbf{n})\left[1 + \Delta(\mathbf{n})\right]$$

$$\langle \mathrm{C}_\ell \rangle = \sum_{\ell_1} M^{-1}_{\ell\ell_1} \left\langle \tilde{\mathrm{C}}_\ell \right\rangle - \frac{4\pi f_1^2}{N f_2}$$

$$\ldots 1)\mathrm{W}_{\ell_2} \begin{pmatrix} \ell & \ell_1 & \ell_2 \\ 0 & 0 & 0 \end{pmatrix}^2$$

- Same approach as JCAP 06 (2017) 026;
- Same data set used for Rayleigh analysys
- Data set 2.15 x larger than JCAP sample:

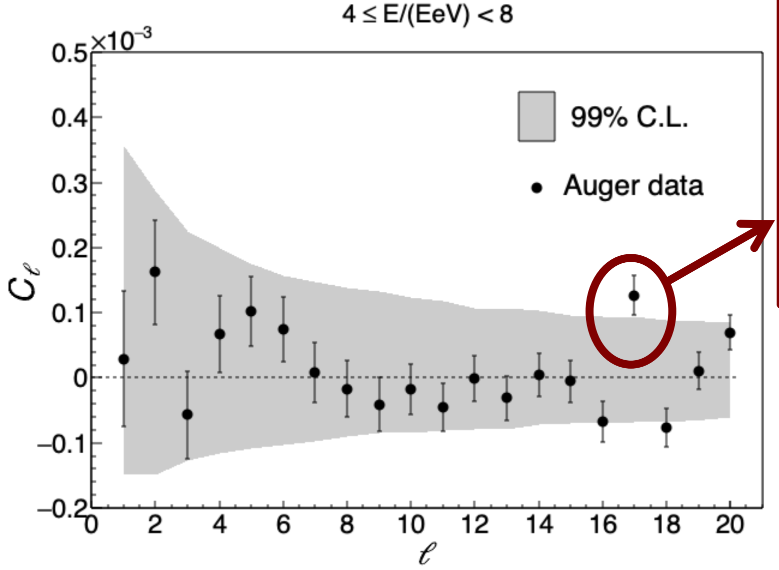

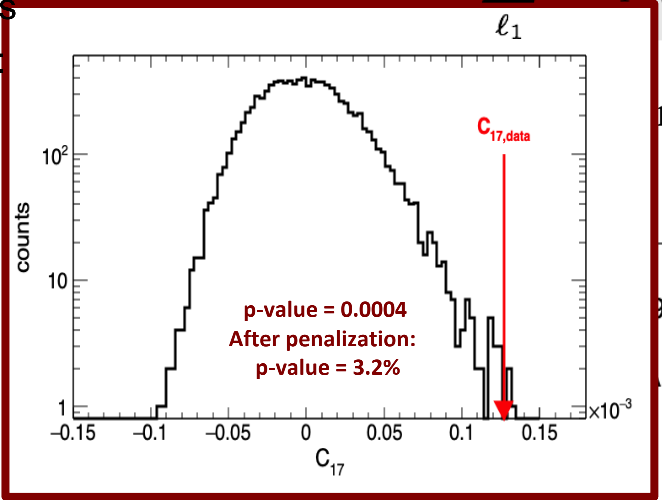

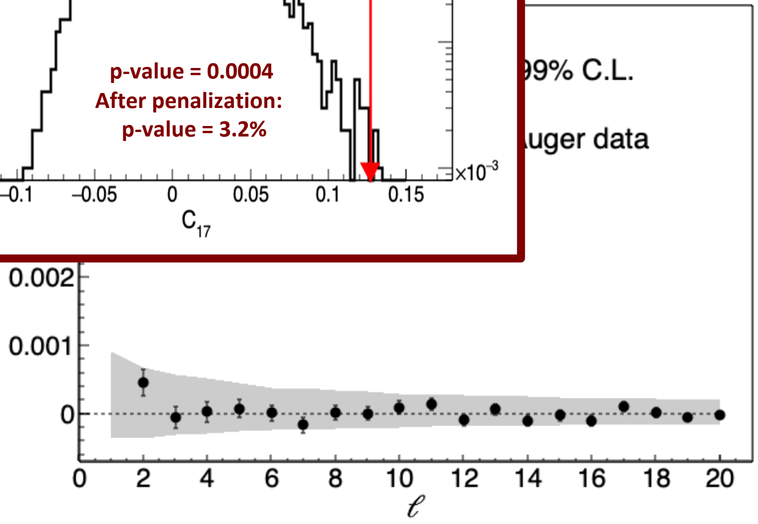

Angular Power Spectrum, splitting the bin above 8 EeV

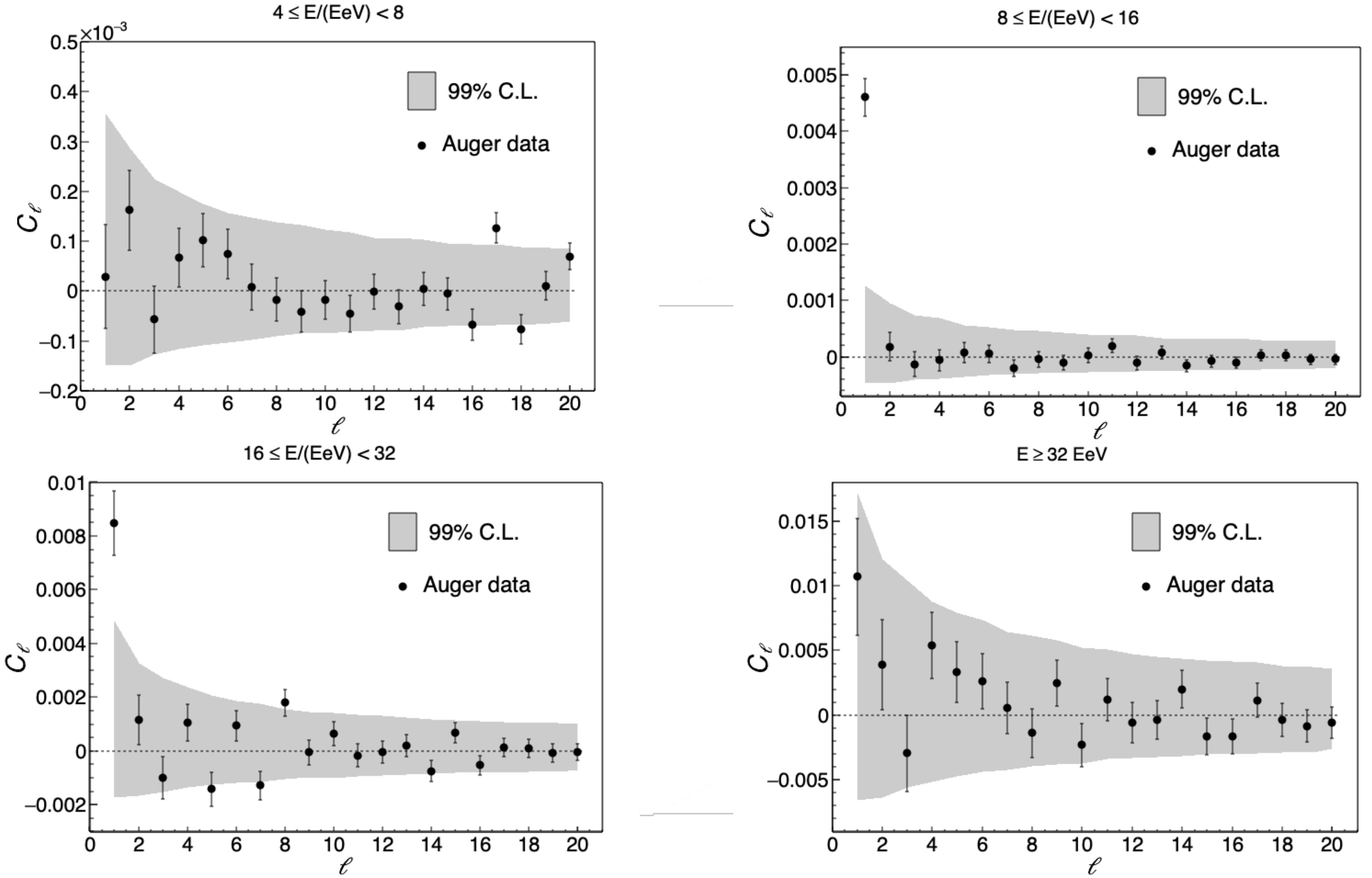

Angular Power Spectrum, splitting the bin above 8 EeV

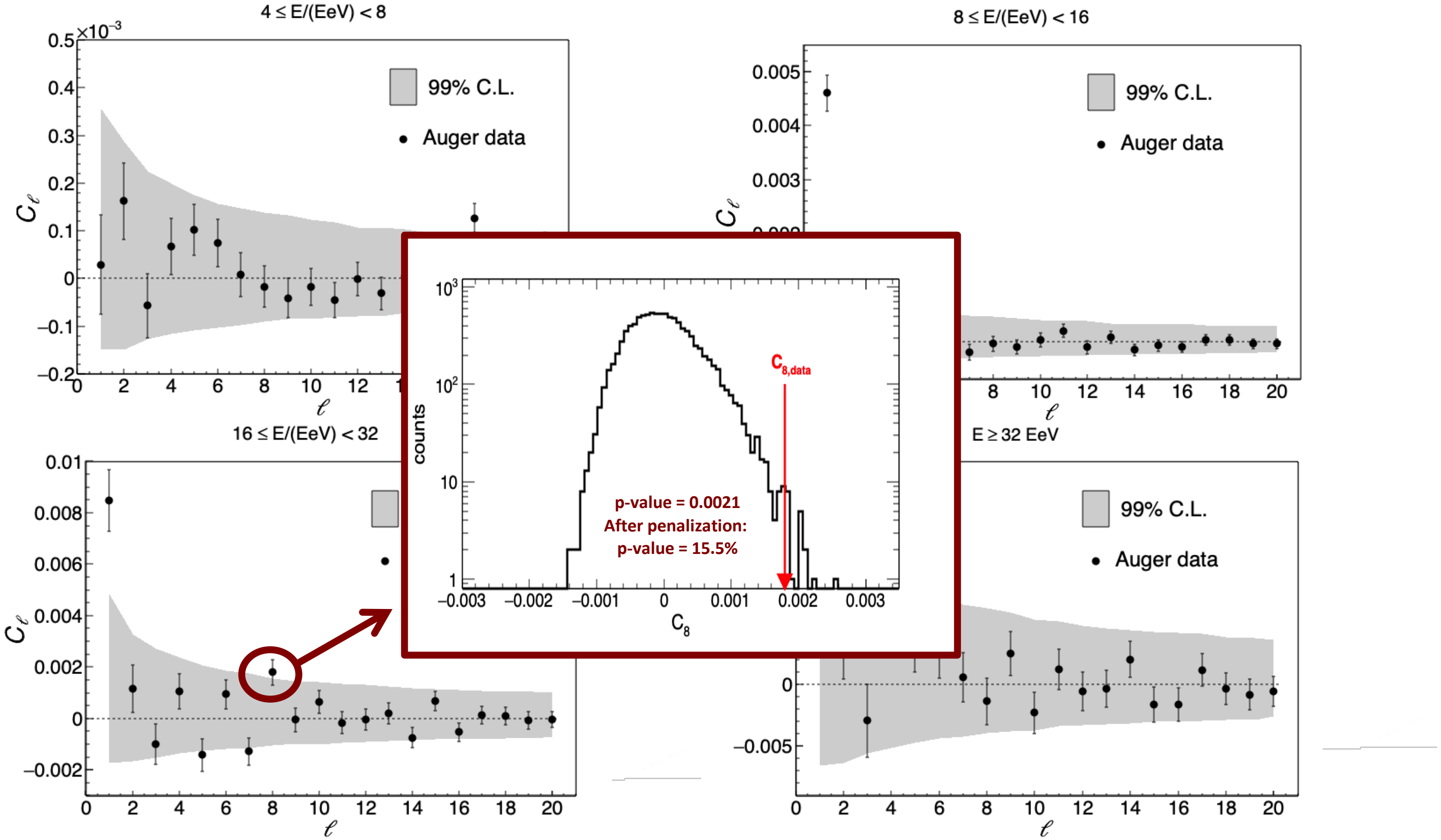

Summary

Rayleigh analysis:

- The statistical significance of the large-scale dipolar modulation observed above 8 EeV has increased to 6.6σ, (p-value = 5.1×10^{-11}).

- The dipolar amplitude increases with energies although there is no clear trend in the change of the dipole direction as a function of energy.
  - Possibly due to the larger relative contribution from nearby sources to the flux at higher energies; Interpretation of the rec. dipole directions requires taking into account the magnetic deflections of the particles during their trajectories.

- Quadrupolar components are not significant in any of the energy bins considered.

Angular power spectrum:

- C_1 increases with energy in agreement with Rayleigh analyses.

- All other multipoles are not significant ➔ C_{17} for 4 < E/EeV < 8 with post-trial p-value = 3.2% and C_8 for 16 < E/EeV < 32 energy bin with post-trial p-value = 15.5%.

Backup

Dipole reconstruction

E (EeV)	N	$d_\perp$	d_z	d	$\alpha_d[^\circ]$	$\delta_d[^\circ]$	$P(\geq r_1^\alpha)$
4-8	106, 290	$0.01^{+0.006}_{-0.004}$	-0.012 ± 0.008	$0.016^{+0.008}_{-0.005}$	97 ± 29	-48^{+23}_{-22}	1.4×10^{-1}
8-16	32, 794	$0.055^{+0.011}_{-0.009}$	-0.03 ± 0.01	$0.063^{+0.013}_{-0.009}$	95 ± 10	-28^{+12}_{-13}	3.1×10^{-7}
16-32	9, 156	$0.072^{+0.021}_{-0.016}$	-0.07 ± 0.03	$0.10^{+0.03}_{-0.02}$	81 ± 15	-43^{+14}_{-14}	7.5×10^{-4}
≥8	44, 398	$0.059^{+0.009}_{-0.008}$	-0.042 ± 0.013	$0.073^{+0.011}_{-0.009}$	95 ± 8	-36^{+9}_{-9}	5.1×10^{-11}
≥32	2, 448	$0.11^{+0.04}_{-0.03}$	-0.12 ± 0.05	$0.16^{+0.05}_{-0.04}$	139 ± 19	-47^{+16}_{-15}	1.0×10^{-2}

was 1.4×10^{-9} (ApJ 2020) and 2.6×10^{-8} (Science 2017)

Corresponds to 6.6σ

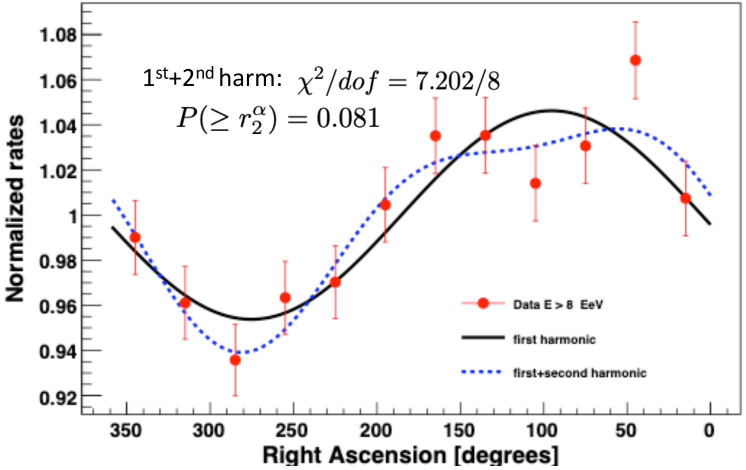

$E \geq 8$ EeV

Smoothed by a top-hat window with 45° of radius

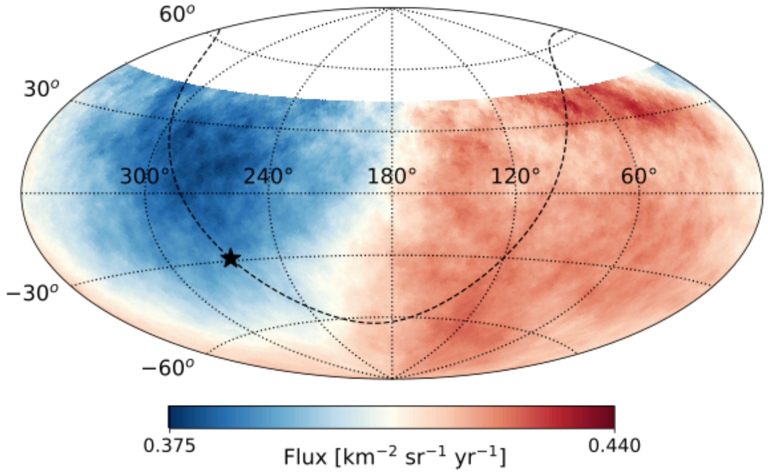

Harmonic analysis in right ascension

Results of the First and Second-harmonic Analyses in R.A

Energy (EeV)	Events	k	a_k^α	b_k^α	r_k^α	$P(\geq r_k^\alpha)$
4-8	106290	1	-0.001 $\pm$ 0.004	0.008 $\pm$ 0.004	0.008	1.4×10^{-1}
		2	0.0006 $\pm$ 0.004	-0.004 $\pm$ 0.004	0.004	6.0×10^{-1}
8-16	32794	1	-0.003 $\pm$ 0.008	0.043 $\pm$ 0.008	0.043	3.1×10^{-7}
		2	0.004 $\pm$ 0.008	0.013 $\pm$ 0.008	0.014	2.2×10^{-1}
16-32	9156	1	0.009 $\pm$ 0.015	0.055 $\pm$ 0.015	0.056	7.5×10^{-4}
		2	0.029 $\pm$ 0.015	-0.017 $\pm$ 0.015	0.034	7.1×10^{-2}
≥ 8	44398	1	-0.004 $\pm$ 0.007	0.046 $\pm$ 0.007	0.046	5.1×10^{-11}
		2	0.013 $\pm$ 0.007	0.008 $\pm$ 0.007	0.015	8.0×10^{-1}
≥ 32	2448	1	-0.07 $\pm$ 0.03	0.06 $\pm$ 0.03	0.087	1.0×10^{-2}
		2	0.070 $\pm$ 0.03	0.034 $\pm$ 0.03	0.078	2.4×10^{-2}

Harmonic analysis in azimuth

Energy (EeV)	k	a_k^ϕ	b_k^ϕ
4-8	1	-0.009 ± 0.004	-0.006 ± 0.004
	2	-0.001 ± 0.004	-0.005 ± 0.004
8-16	1	-0.014 ± 0.008	-0.016 ± 0.008
	2	-0.009 ± 0.008	0.010 ± 0.008
16-32	1	-0.002 ± 0.015	-0.036 ± 0.015
	2	0.016 ± 0.015	-0.005 ± 0.015
≥8	1	-0.009 ± 0.007	-0.023 ± 0.007
	2	-0.002 ± 0.007	0.009 ± 0.007
≥32	1	0.002 ± 0.029	-0.064 ± 0.029
	2	0.019 ± 0.029	0.044 ± 0.029

ApJ 2018, E > 8 EeV

$$b_1^\phi = -0.014 \pm 0.008$$

a_1^ϕ consistent with zero as expected

Dipole reconstruction E > 8 EeV

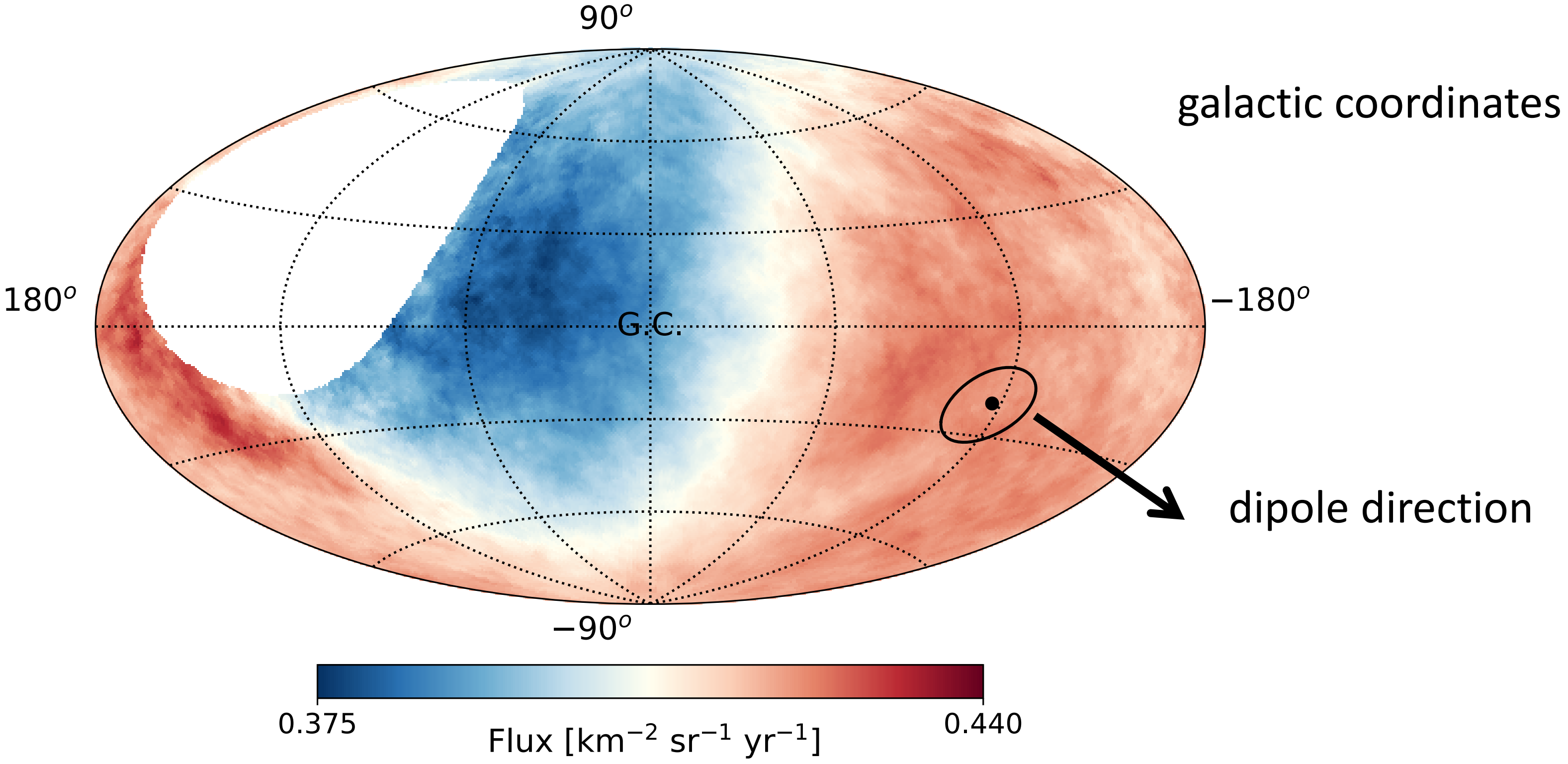

Dipole points to $(\mathrm{l}, \mathrm{b}) = \left(-117^{\circ}, -21^{\circ}\right) \sim 115^{\circ}$ away from the direction of the Galactic center

Dipole reconstruction

Ratio between observed and expected events in windows of 45º

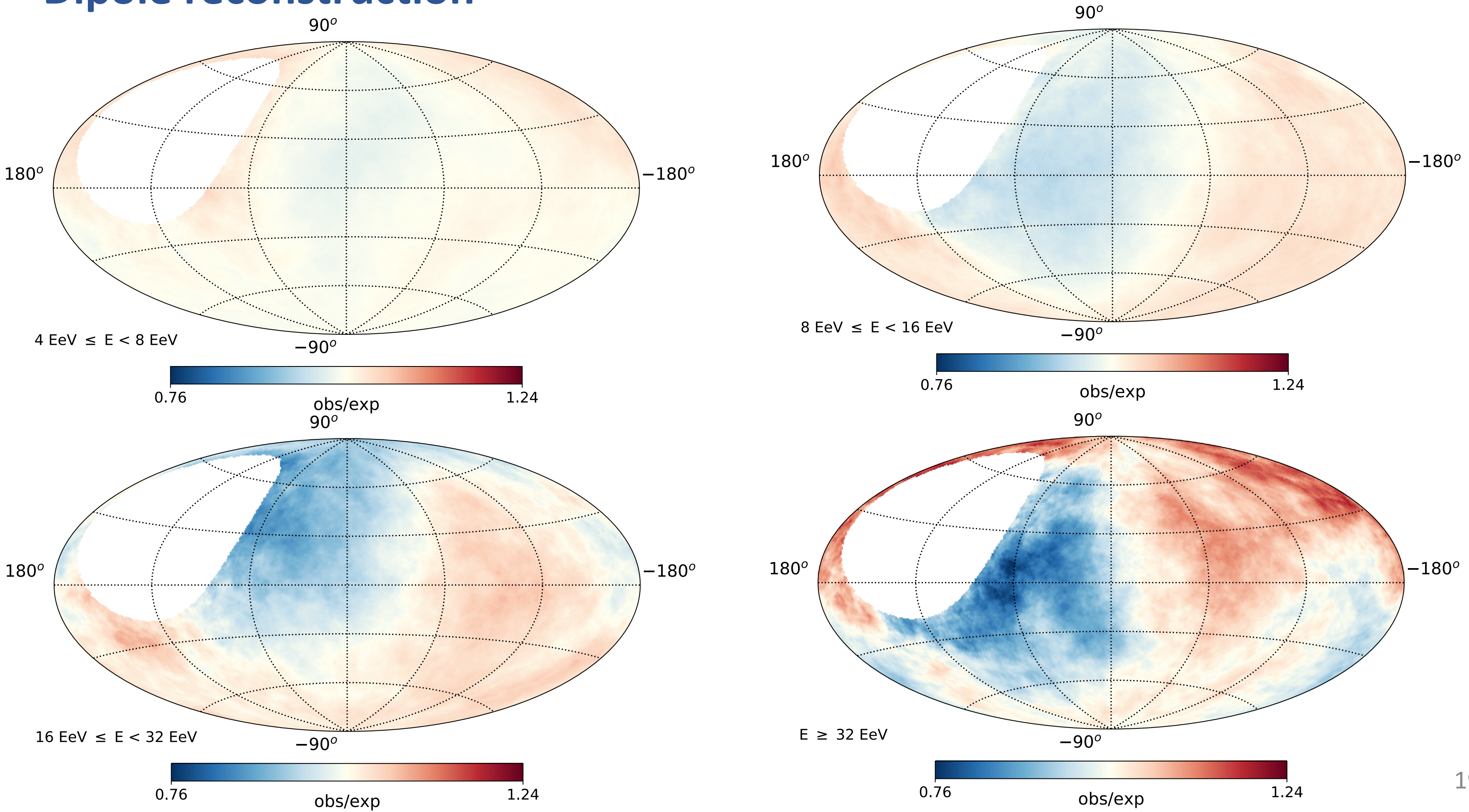

Dipole contours

ICRC 2019

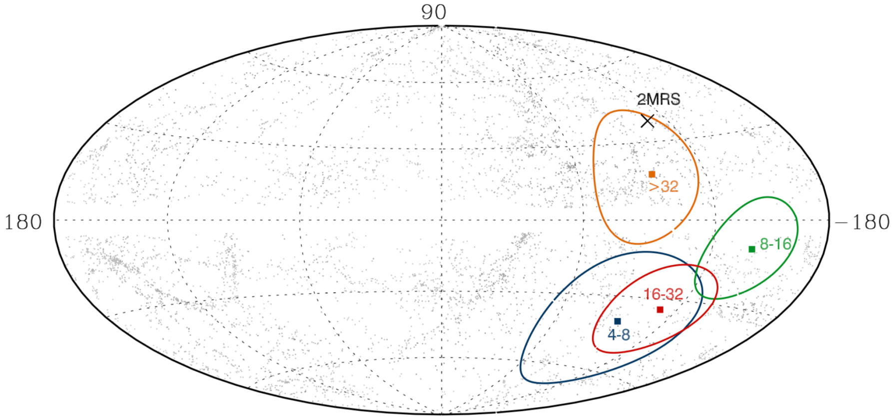

This work

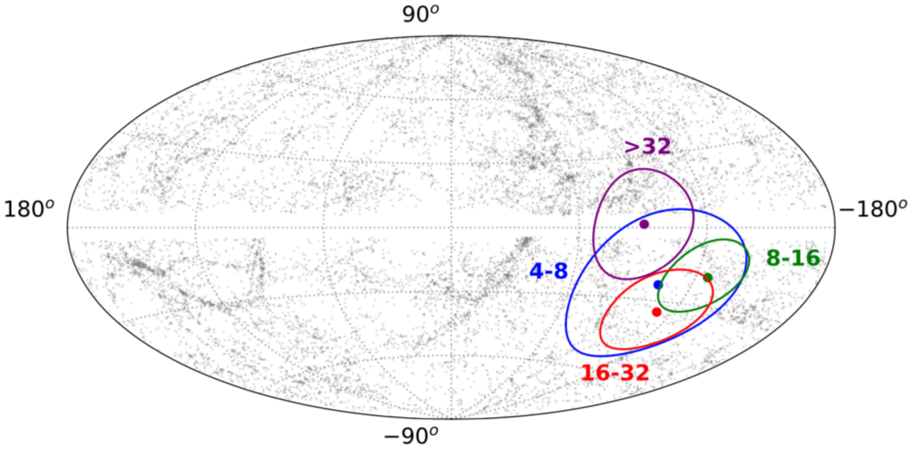

Dipole contours

ICRC 2019

Energy [EeV] interval	median	N	$d_\perp$	d_z	d	α_d [°]	δ_d [°]
4 - 8	5.0	88,325	$0.010^{+0.007}_{-0.004}$	-0.016 ± 0.009	$0.019^{+0.009}_{-0.006}$	69 ± 46	-57^{+24}_{-20}
≥ 8	11.5	36,928	$0.060^{+0.010}_{-0.009}$	-0.028 ± 0.014	$0.066^{+0.012}_{-0.008}$	98 ± 9	-25 ± 11
8 - 16	10.3	27,271	$0.056^{+0.012}_{-0.010}$	-0.011 ± 0.016	$0.057^{+0.014}_{-0.008}$	97 ± 12	-11 ± 16
16 - 32	20.2	7,664	$0.075^{+0.023}_{-0.018}$	-0.07 ± 0.03	$0.10^{+0.03}_{-0.02}$	80 ± 17	-44 ± 14
≥ 32	39.5	1,993	$0.13^{+0.05}_{-0.03}$	-0.09 ± 0.06	$0.16^{+0.06}_{-0.03}$	152 ± 19	-34^{+19}_{-20}

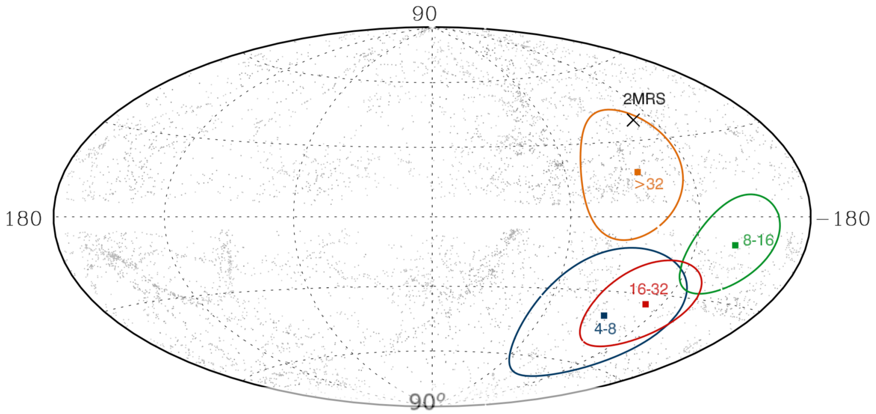

This work

E (EeV)	N	$d_\perp$	d_z	d	α_d[°]	δ_d[°]	P($\geq r_k^\alpha$)
4-8	106, 290	$0.01^{+0.006}_{-0.004}$	-0.012 ± 0.008	$0.016^{+0.008}_{-0.005}$	97 ± 29	-48^{+23}_{-22}	1.4×10^{-1}
8-16	32, 794	$0.055^{+0.011}_{-0.009}$	-0.03 ± 0.01	$0.063^{+0.013}_{-0.009}$	95 ± 10	-28^{+12}_{-13}	3.1×10^{-7}
16-32	9, 156	$0.072^{+0.021}_{-0.016}$	-0.07 ± 0.03	$0.10^{+0.03}_{-0.02}$	81 ± 15	-43^{+14}_{-14}	7.5×10^{-4}
≥8	44, 398	$0.059^{+0.009}_{-0.008}$	-0.042 ± 0.013	$0.073^{+0.011}_{-0.009}$	95 ± 8	-36^{+9}_{-9}	5.1×10^{-11}
≥32	2, 448	$0.11^{+0.04}_{-0.03}$	-0.12 ± 0.05	$0.16^{+0.05}_{-0.04}$	139 ± 19	-47^{+16}_{-15}	1.0×10^{-2}

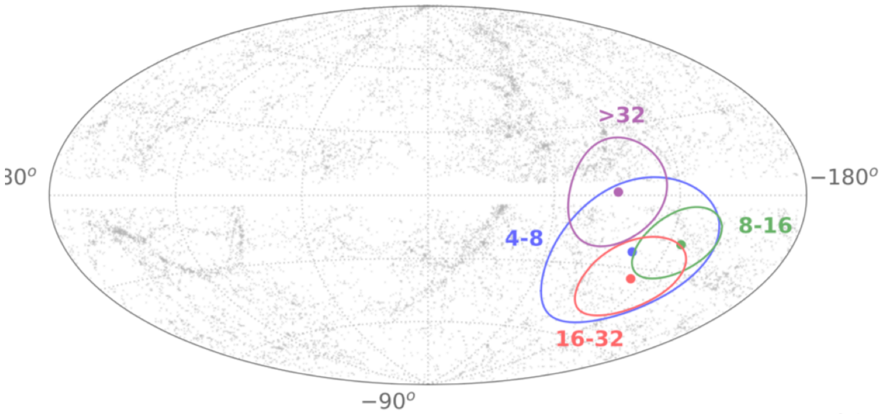

Dipole amplitude evolution with energies

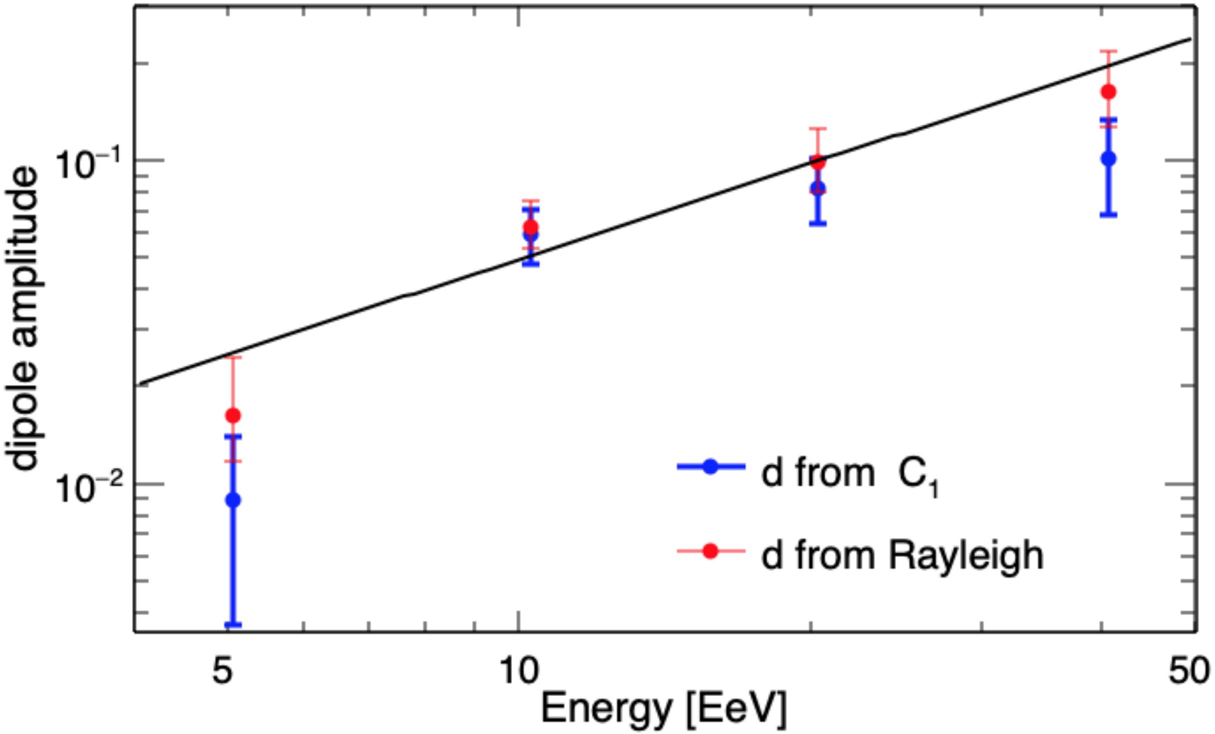

Solar and anti-sideral analyzes

Energy (EeV)	Solar		Anti-sidereal	
	r_1	$P(\geq r_1)$	r_1	$P(\geq r_1)$
4 - 8	0.004	0.66	0.006	0.41
8-16	0.004	0.89	0.007	0.65
16-32	0.017	0.53	0.02	0.35
≥ 8	0.003	0.89	0.01	0.32
≥ 32	0.013	0.90	0.01	0.93

No statistical significant flux modulation indicating that corrections were accurately accounted

Variation of the array size

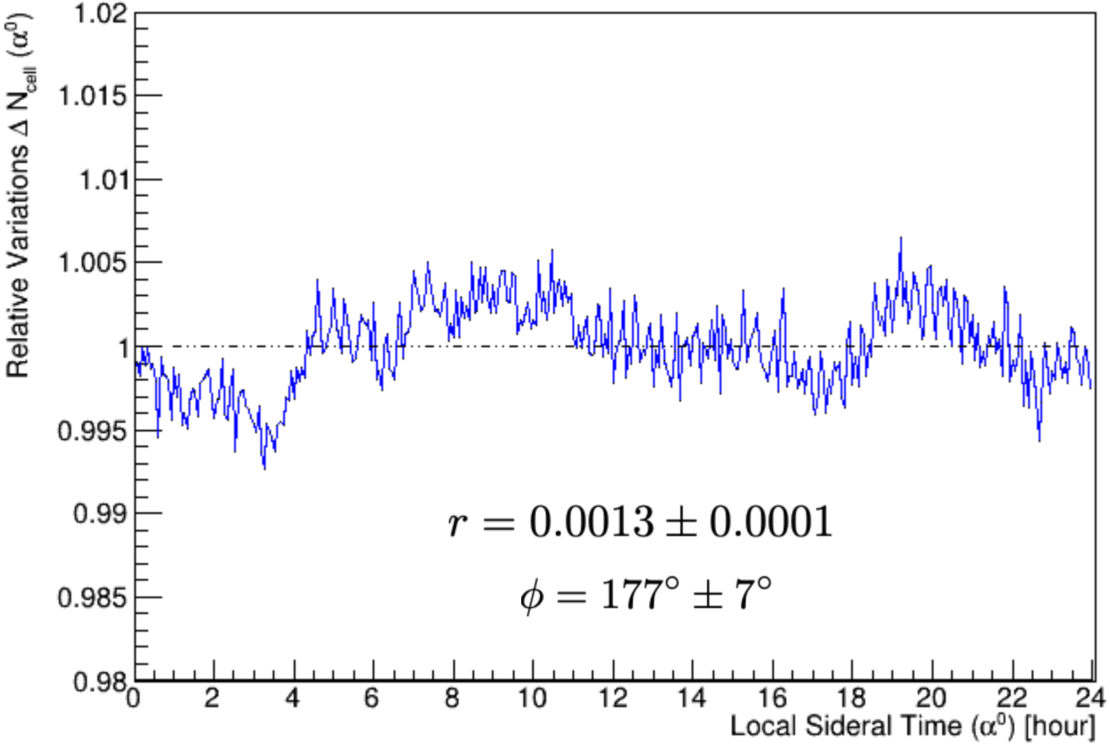

Quadrupolar amplitudes $Q \equiv \sqrt{\sum_{ij} Q_{ij}^2 / 9}$

Directly related to the usual angular power spectrum moments $Q^2 = (50/3) C_2 / C_0$

$4 \le E/\mathrm{EeV} < 8$

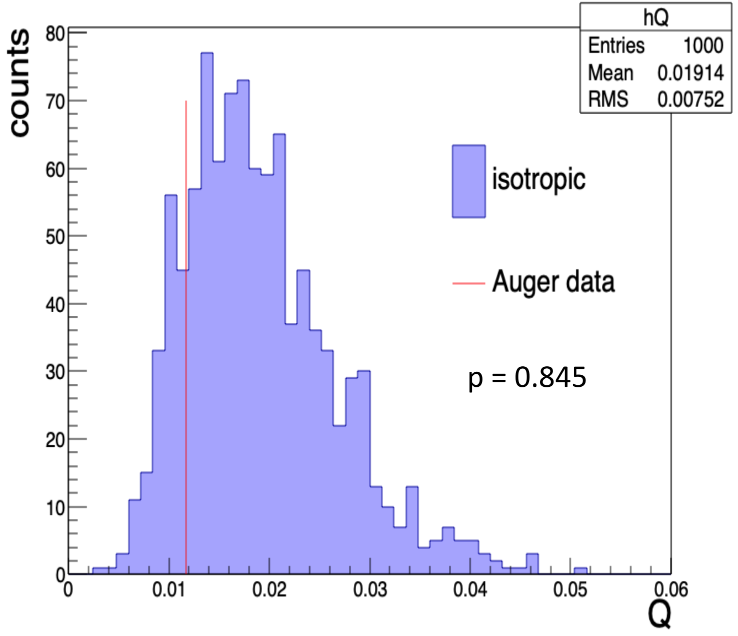

$E \ge 8$ EeV

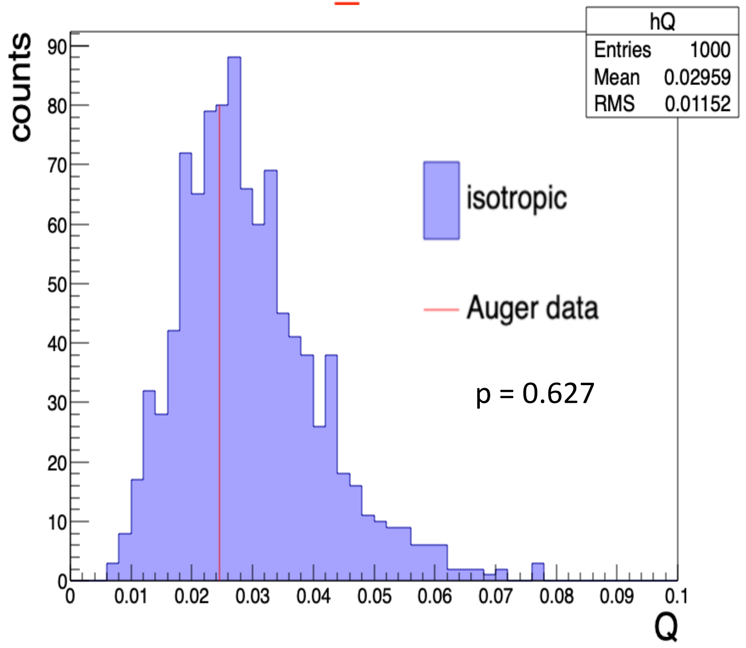

Quadrupolar amplitudes

$$Q \equiv \sqrt{\sum_{ij} Q_{ij}^2 / 9}$$

$8 \leq E/\mathrm{EeV} < 16$

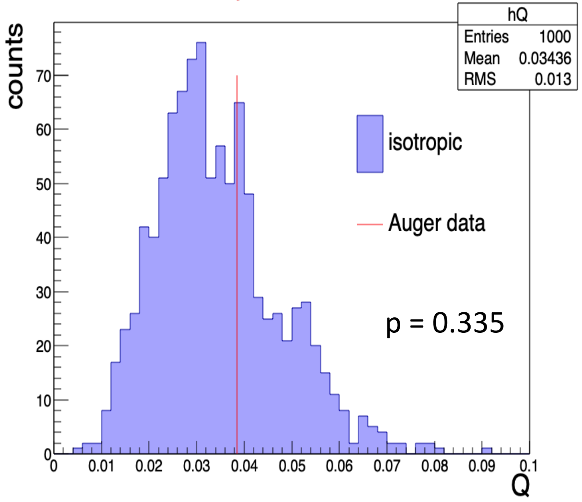

$16 \leq E/\mathrm{EeV} < 32$

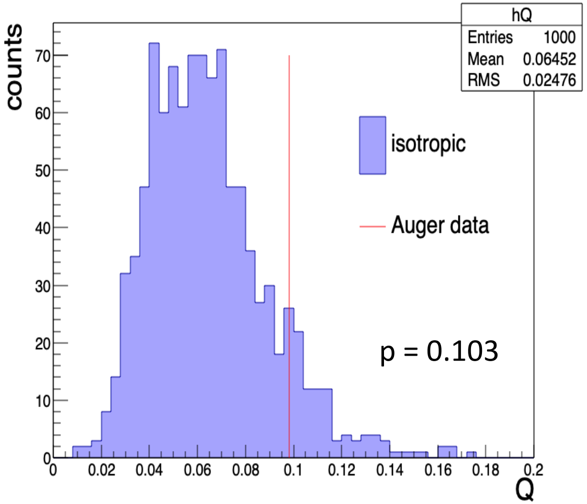

$E \geq 32\mathrm{EeV}$

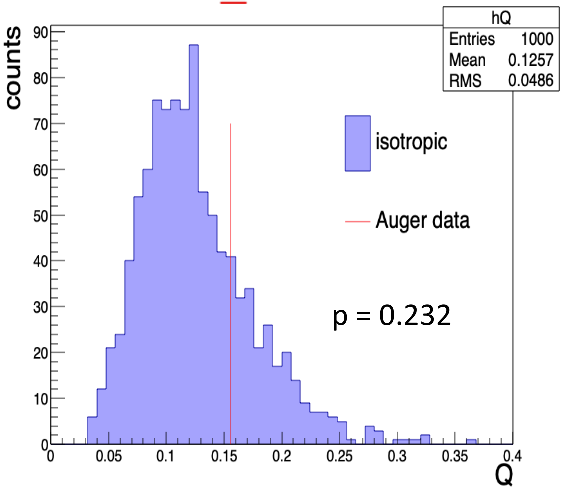

Quadrupolar components

$4 \leq E/\mathrm{EeV} < 8$

- 1000 simulations of isotropic skies with same number of events in data for each energy bin

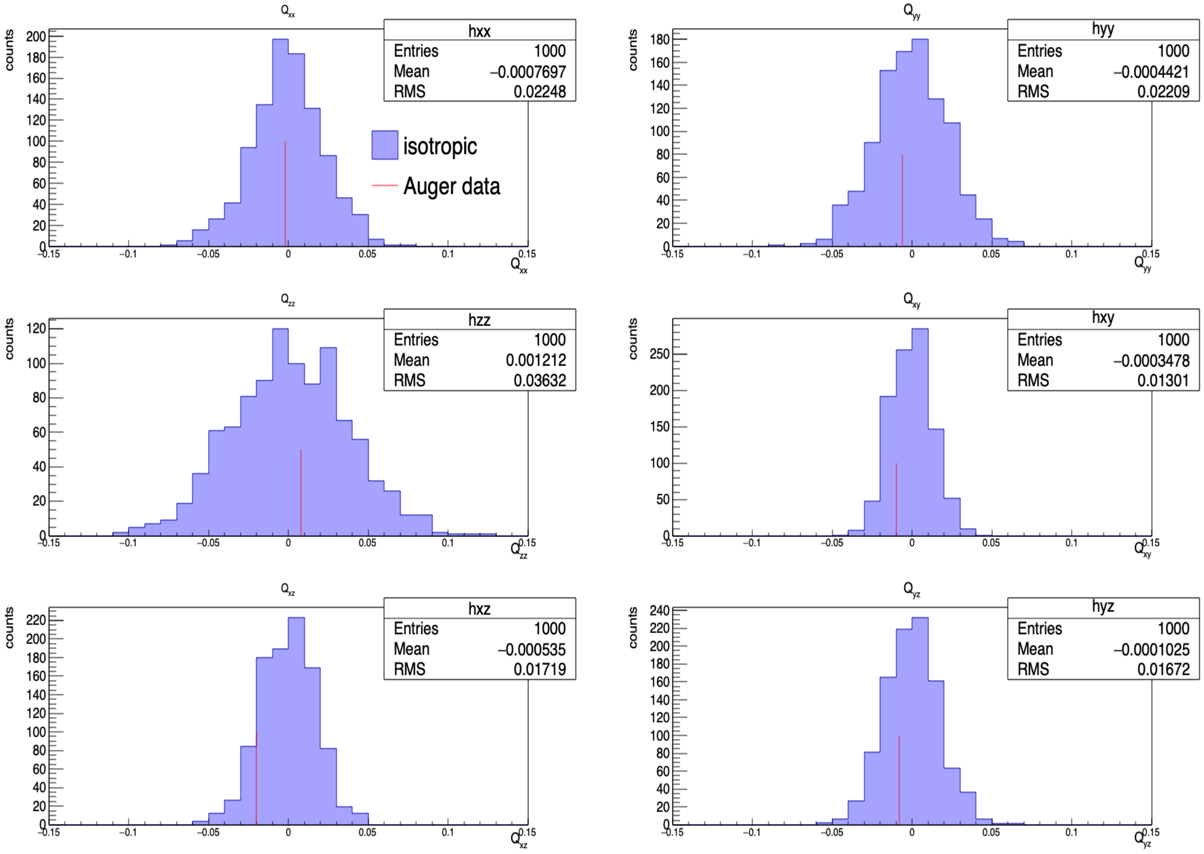

Quadrupolar components p-values

$E \geq 8$ EeV

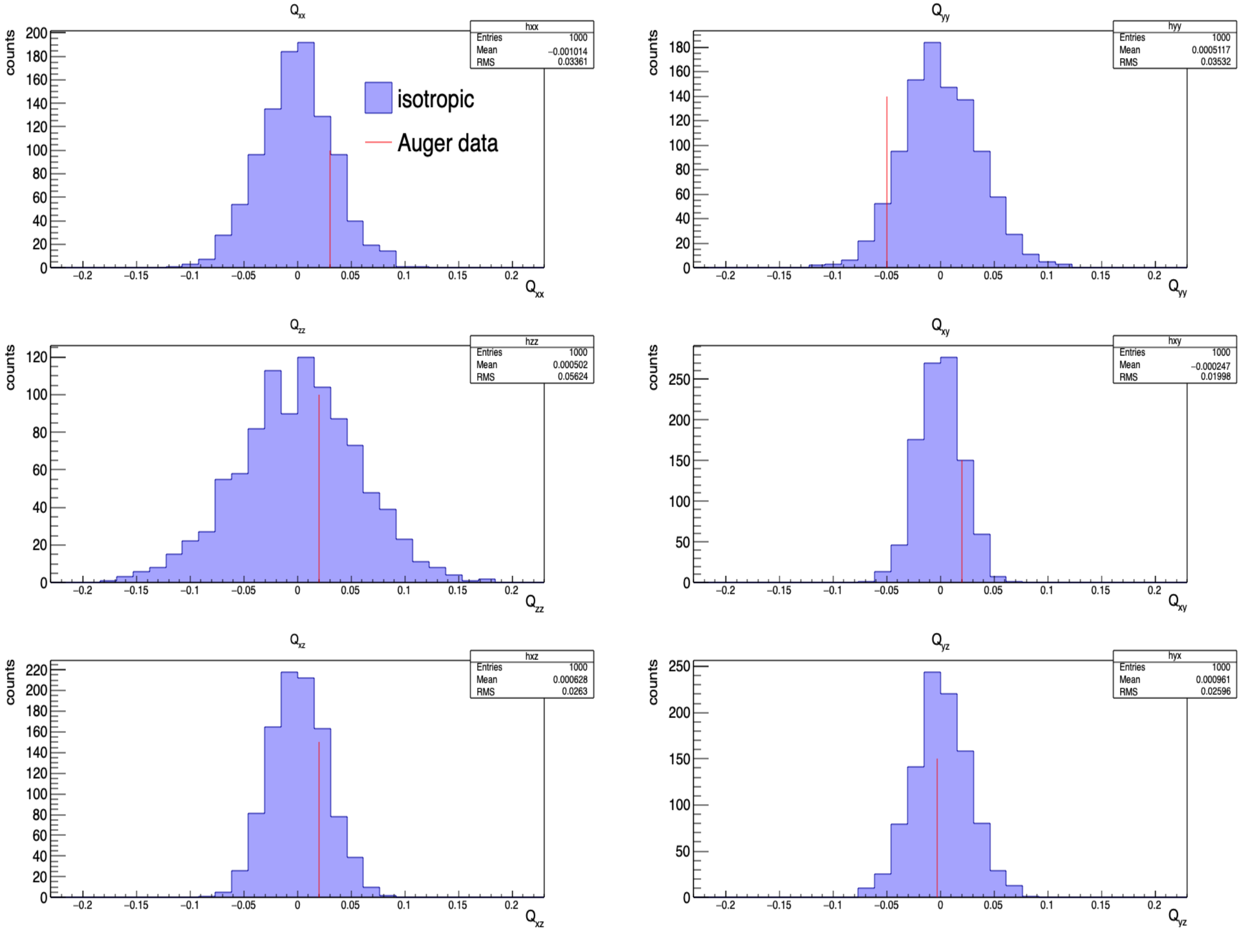

Quadrupolar components p-values

$8 \leq E/\mathrm{EeV} < 16$

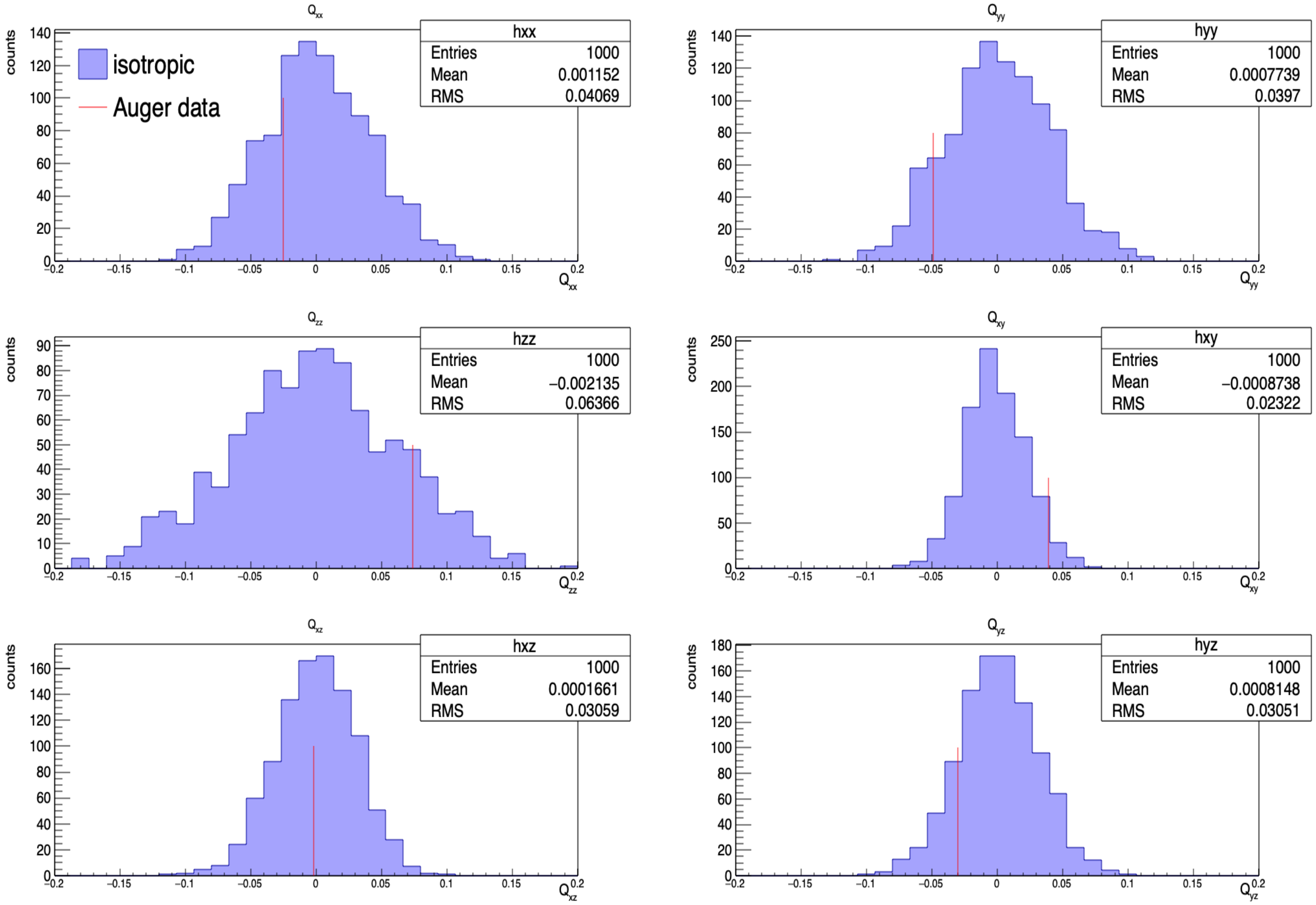

Quadrupolar components p-values

$16 \leq E/\mathrm{EeV} < 32$

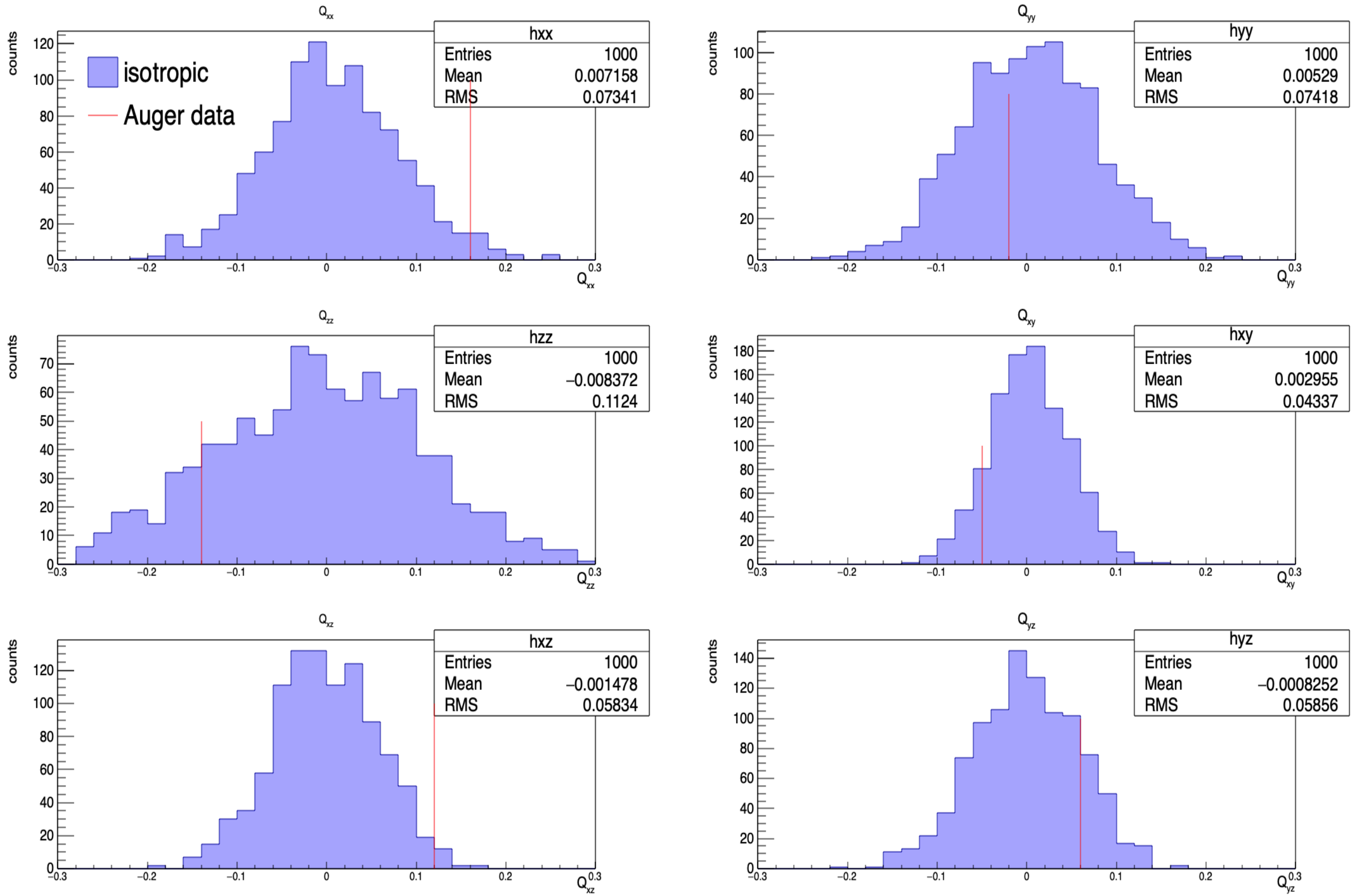

Quadrupolar components p-values

$E \geq 32\mathrm{EeV}$

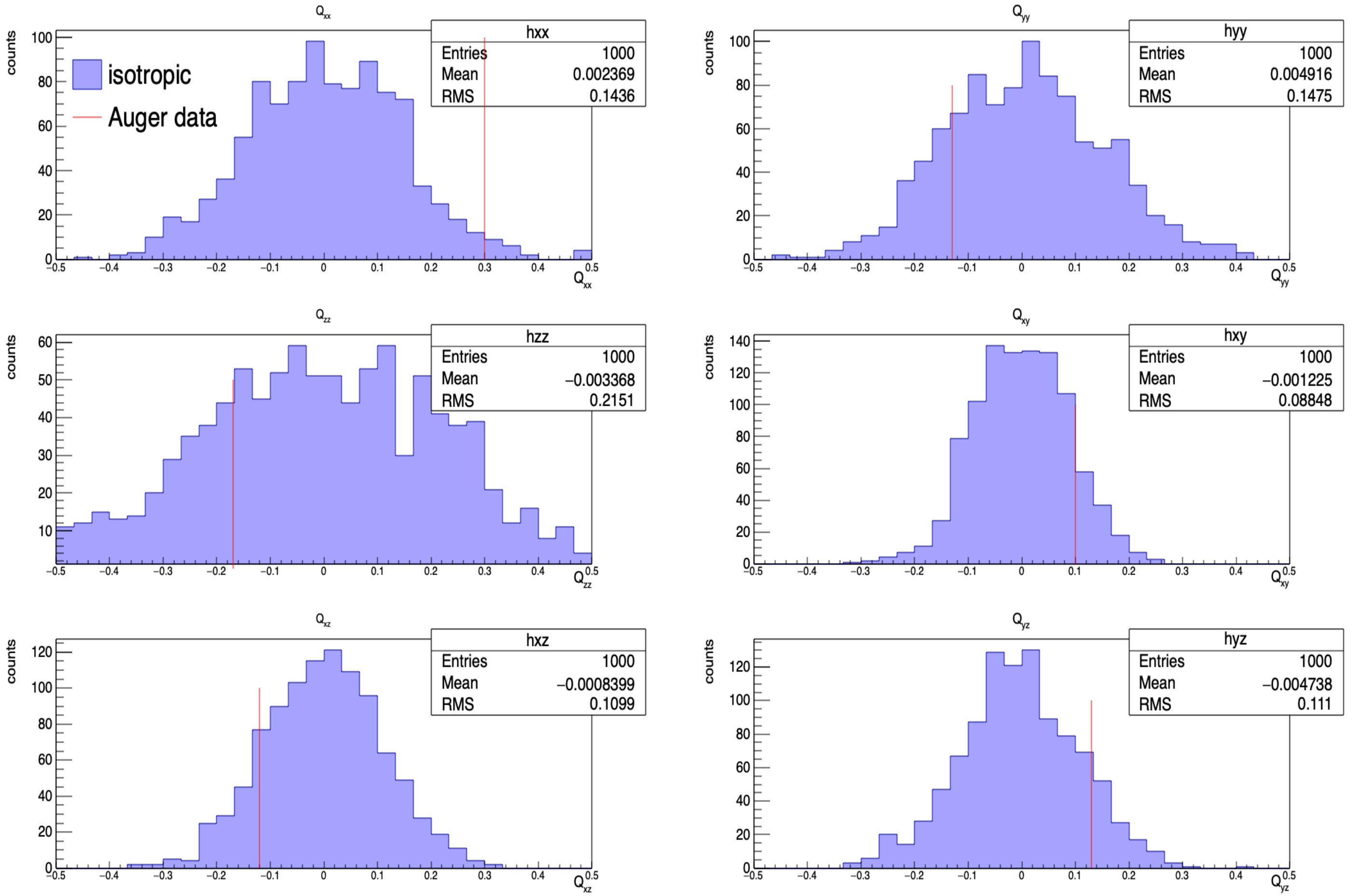

Quadrupolar components

Correlations between quadrupolar and dipolar components

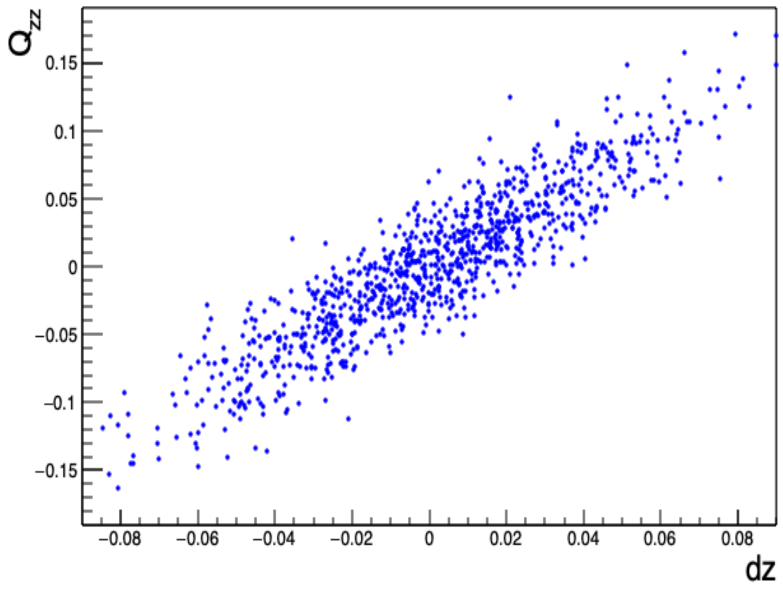

$$\rho(d_z, Q_{zz}) = 0.91$$

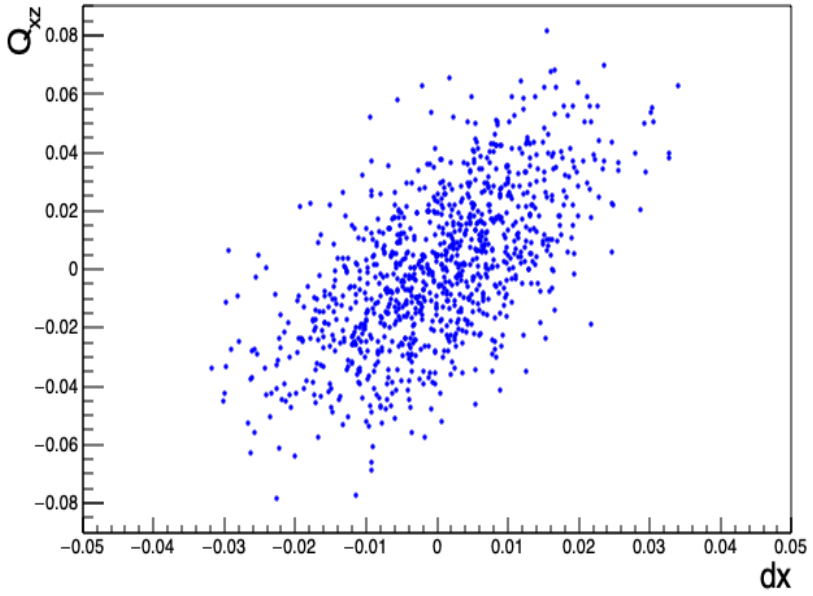

$$\rho(d_x, Q_{xz}) = \rho(d_y, Q_{yz}) = 0.63$$